Simulation of Cross Flow Induced Vibration

Eric Williams, P.Eng
Graduate Student, University of New Brunswick, Canada
Andrew Gerber, PhD, P.Eng
Associate Professor, University of New Brunswick, Canada
Marwan Hassan, PhD, PEng
Assistant Professor, University of New Brunswick, Canada

Abstract

This paper describes the development of a tool for predicting the vibration response of elastically mounted bluff bodies (in this case a cylindrical tube or tube arrays) excited by fluid forces in cross-flow. The modelling approach utilizes computational-fluid-dynamics (CFD) to model the transient behaviour of the fluid flow with explicit coupling to a structural model of the bluff body. The structural model represents the inertial, damping and spring characteristics of the bluff body. The paper presents preliminary validation of the model for laminar and turbulent flow in single tube arrangements. Validation against experiment emphasizes comparison with mean and RMS drag and lift values, along with Strouhal number to measure fluid vortex-shedding frequency. The results represent a preliminary step in the development of a methodology to extract force coefficients, obtained directly by coupling CFD and FEA, for introduction into unsteady structural (vibration) response models applicable to large tube arrays.

Introduction

As fluid flows through an array of elastic tubes, such as in a shell and tube heat exchanger, the tubes deflect due to drag and lift forces, generated by vortex shedding, turbulence and fluidelastic instability. This is known as flow-induced vibration. At low flow velocities, the fluid flow around a given tube acts as a damper, limiting the amplitude of motion. As the flow velocity increases so do the pressure and shear forces, increasing the net lift and drag forces on the tubes. Eventually, at some critical velocity, the energy input from these external fluid forces exceeds the structural damping and the amplitude of the tube vibration rises dramatically, particularly in the cross-flow direction. This phenomenon is known as fluidelastic instability. In typical heat exchangers, the tubes are closely spaced which has the effect of reducing vortex induced forces.

Fluidelastic instability is caused by the strong feedback between fluid forces and the structural motion. The fluid forces cause the tube to displace, which in turn changes the flow patterns and hence the net pressure around the tube. This change in pressure in turn provokes a change in the tube displacement and the cycle repeats. Several models have been developed to predict the fluidelastic instability in tube arrays. One of the most comprehensive to date was the Unsteady Flow Theory developed by Chen [1] in which the forces acting on a single tube in an array are a function of the position, velocity and acceleration of every tube in the array. A series of coefficients are used to scale the individual tube effects to predict the total force on any tube. Finally, the contributions of each tube to the forces are assumed to sum linearly. In an array of N tubes, the forces acting on tube j are calculated:

$$Fx_j = -\sum_{k=1}^{N}\left\{\left[\overline{\alpha}_{jk}\frac{\partial^2 u_k}{\partial t^2}+\overline{\alpha}'_{jk}\frac{\partial u_k}{\partial t}+\overline{\alpha}''_{jk}u_k\right]+\left[\overline{\sigma}_{jk}\frac{\partial^2 v_k}{\partial t^2}+\overline{\sigma}'_{jk}\frac{\partial v_k}{\partial t}+\overline{\sigma}''_{jk}v_k\right]\right\}$$

$$Fy_j = -\sum_{k=1}^{N}\left\{\left[\overline{\tau}_{jk}\frac{\partial^2 u_k}{\partial t^2}+\overline{\tau}'_{jk}\frac{\partial u_k}{\partial t}+\overline{\tau}''_{jk}u_k\right]+\left[\overline{\beta}_{jk}\frac{\partial^2 v_k}{\partial t^2}+\overline{\beta}'_{jk}\frac{\partial v_k}{\partial t}+\overline{\beta}''_{jk}v_k\right]\right\}$$

where Fx_j and Fy_j are the forces acting on tube j in the x (in-flow) and y (cross-flow) directions, N is the total number of tubes in the array, u and v are the velocities in the x and y directions and k is the index of the tube of influence. For a single tube array, $j = k = 1$. The twelve Greek symbols, $\overline{\alpha}, \overline{\sigma}, \overline{\tau}, \overline{\beta}$, etc., are the coefficients of interest and are highly non-linear. These coefficients are themselves functions of pitch-to-diameter ratio, Reynolds number, reduced velocity, array geometry, relative roughness and many other variables. As an example, experimental work by Tanaka and Takahara produced the following graph of $\overline{\alpha}'_{11}$ at various reduced velocities (U_r) for a square array with pitch-to-diameter ratio of 1.33 [2].

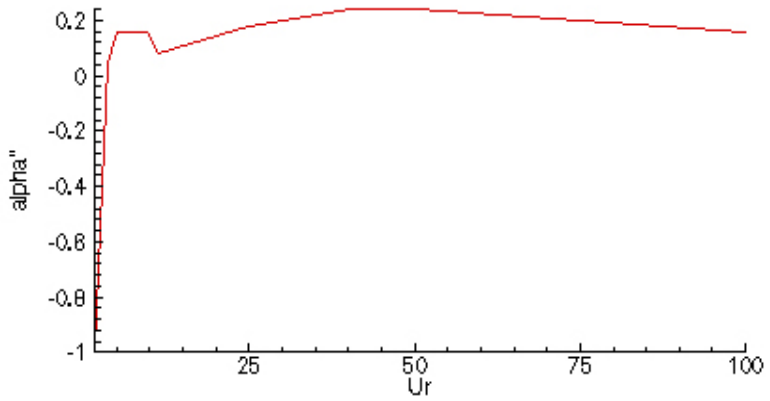

Figure 1. Experimental Fluid Force Coefficient $\overline{\alpha}'_{11}$

The objective of this project is to extract the Unsteady Flow Theory model coefficients from numerical predictions rather than costly experiments, where fluid forces must be deduced indirectly from tube displacement measurements. This approach provides a more complete model for fluidelastic instability in tube arrays, where force coefficients can be calculated directly. Then the obtained force coefficients can be utilized in Finite Element codes to predict the tube's fretting wear damage. To the authors' knowledge this is the first attempt to extract the Unstead Flow Theory model coefficients using CFD coupled with FEA.

To model the fluid-structure interaction, the CFD software CFX-TASCflow 2.12 is used to predict the fluid pressure and shear forces around each tube at each time step. The forces are then integrated around the tube to generate net lift and drag forces. The force components are passed to a dynamic tube response model to calculate the new tube position, including the effects of tube stiffness, structural damping and inertia. The new position is returned to the CFD code and the nodes attached to the tube are displaced accordingly. The remaining nodes in the interior of the domain are displaced through the solution of a Laplacian displacement equation, which uses the tube surface displacements as boundary conditions.

To validate the model, it has first been tested as a single rigid tube at low Reynolds numbers. Once the mean and RMS drag, RMS lift and Strouhal numbers were matched to experimental values, and the solution was found to be grid and time step independent, the model was expanded to include the effects of elasticity. Future work will include adding neighboring tubes and validating against experimental data for two adjacent, elastic tubes.

Governing Equations

Conservation Equations for Fluid Flow and Moving Grid

By dividing the calculated grid deflection by the time step, a grid (or mesh) velocity can be calculated. This velocity, u_{mj}. is used in conjunction with an Arbitrary Lagrangian-Eulerian (ALE) description of the governing equations [3]. In this form the advection terms include the mesh velocity along with the fluid advection velocity. This results in a modified form of the mass conservation and Navier-Stokes momentum equations as follows.

Mass Conservation:

$$\frac{\partial \rho}{\partial t} + \frac{\partial \rho (u_j - u_{mj})}{\partial x_j} = 0$$

Momentum:

$$\frac{\partial \rho u_i}{\partial t} + \frac{\partial \rho u_i (u_j - u_{mj})}{\partial x_j} = -\frac{\partial \tau_{ij}}{\partial x_j} - \frac{\partial P}{\partial x_i}$$

where u_m is the grid velocity (m/s) and τ_{ij} is the deformation tensor. This form of the governing equations allows conservative fluid flow calculations with mesh adaptation in tune.

Small-scale turbulence is not expected to play a significant role in force generation, therefore a two-equation Reynolds Averaged Navier-Stokes (RANS) turbulence model has been used for simplicity rather than a transient specific model such as Large Eddy Simulation (LES) or Detached-Eddy Simulation (DES). The point of flow separation is of importance when predicting the shear and pressure forces acting on a tube, and therefore the k-ε epsilon turbulence model would not be expected to accurately predict the separation point. To better account for separation the Shear Stress Transport (SST) turbulence model is used. It uses a k-ω formulation in the near wall region; its conservation equations are shown below. To account for the moving grid, the turbulence equations are also cast in ALE form.

k-equation:

$$\frac{\partial \rho k}{\partial t} + \frac{\partial \rho k (u_j - u_{mj})}{\partial x_j} = P_k - \beta^* \rho k \omega + \frac{\partial}{\partial x_j}\left[\left(\mu + \frac{\mu_t}{\sigma_k}\right)\frac{\partial k}{\partial x_j}\right]$$

ω-equation:

$$\frac{\partial \rho \omega}{\partial t} + \frac{\partial \rho \omega (u_j - u_{mj})}{\partial x_j} = \alpha \frac{\omega}{k} P_k - \beta \rho \omega^2 + \frac{\partial}{\partial x_j}\left[\left(\mu + \frac{\mu_t}{\sigma_\omega}\right)\frac{\partial \omega}{\partial x_j}\right]$$

In these equations P_k is the production rate of turbulence. The SST model incorporates a transformation between the *k*-ε model in the free stream regions of the flow, and the *k*-ω model in the near wall regions of the flow. Additional modifications are used to prevent the over-generation of eddy-viscosity in regions of high recirculation, such as behind the tube. The interested reader is directed to a more complete description in the CFX-TASCflow Theory Manual [4]. The reader will also find a complete description of the values used for $\alpha, \beta^*, \beta, \sigma_k$ and σ_ω in the turbulent transport equations.

Equations Governing Tube Motion

To calculate the response of the tube in the lift and drag directions, two independent, second order equations of motion are solved.

$$m\ddot{x} + c\dot{x} + kx = F_x$$
$$m\ddot{y} + c\dot{y} + ky = F_y$$

where the forces F_x and F_y are the total drag and lift forces acting on the tube and *m*, *c* and *k* are the tube mass per unit length, structural damping coefficient and spring constant respectively.

Equations Governing Grid Motion

Once the structural code determines the response of the tube, the nodes on the tube surface are moved to the new position and the remaining nodes are moved according to a Laplacian diffusion solution, where in 2D:

$$\frac{\partial}{\partial x_j}\left(\frac{\partial x'}{\partial x_j}\right)=0 \quad \frac{\partial}{\partial x_j}\left(\frac{\partial y'}{\partial x_j}\right)=0$$

and

$$x'=x-x^o \quad y'=y-y^o$$

Here x' and y' are the change in position in the x and y directions, x and y are the new nodal coordinates, and x^o and y^o are the old nodal coordinates. With the displacements of the tube and domain boundaries used as boundary conditions, the diffusion equations can be solved for the displacement field throughout the grid, which is used to determine the new node positions.

Problem Description

Fluid Flow Model

For the present work the flow domain is rectangular and encompasses a single tube. CFX-Hexa was used to generate a structured multi-block mesh around a tube of diameter 0.016 m. To minimize computational effort two-dimensional flow is assumed by imposing symmetry conditions on planes along the tube axis. This assumption is made despite the fact that vortex shedding transitions to 3D at a Reynolds number of approximately 200 [5]. It is assumed that in an array of tubes the vortex shedding forces are minimal due to the proximity of the neighboring tubes and relative strength of the instability forces. Furthermore, for the initial model validation where a Reynolds number of 100 is used, the 2D approximation is valid for even a single tube.

The domain, shown in Figure 2, is 21 diameters wide (therefore blockage effects are minimal), with the tube at the center shown as solid black. The inlet region is 13 diameters upstream and the outlet region 59 diameters downstream. The working fluid is air at STP, and the inlet velocity is specified to obtain the appropriate Reynolds number. The outlet has a specified constant pressure of zero and the side walls are specified as zero flux. A zero-slip wall boundary condition is assigned to the tube, which is specified as smooth. To control the mesh motion the user must specify regions identifying "frozen-nodes" and "moved-nodes". The "frozen-nodes" region includes all nodes that will be static, while the "moved-nodes" region includes all nodes, which are attached to the moving surface and will have a predicted displacement. In this case the side walls, inlet and outlet are assigned to be "frozen-nodes" and the tube surface is assigned as "moved-nodes". The remaining nodes along the symmetry regions and in the interior are free to move in response to the "moved-nodes" displacements.

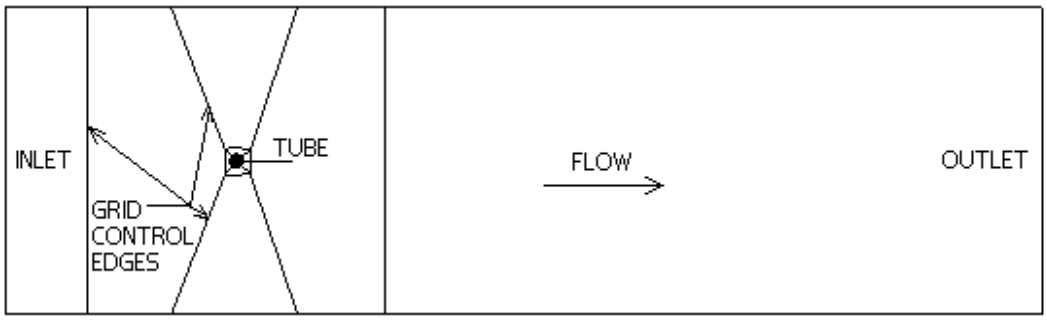

Figure 2. Fluid Domain

Tube Model

The tube has been modeled as a two degree-of-freedom system with independent responses in x - the drag direction, and y - the lift direction. As discussed in the introduction, the response is assumed to be two-dimensional with symmetry along the tube axis. The following properties are applied:

k - Stiffness is 4334.73 (N/m)

ξ - Structural damping is 0.01 or 1%, giving a damping coefficient of 0.46 (Ns/m)

m - Mass per unit length is 0.122 (kg/m)

f_1 - Natural frequency is 30.0 (Hz)

The initial conditions of the tube are zero displacement and velocity. At each time step the structural code calculates the new tube position using the Central Difference Method based on the fluid forces passed from CFX-TASCflow.

Solution Procedure

Although this is a transient problem, the problem is first run as a steady-state calculation to initialize flow conditions for start-up of the transient simulation. To initiate vortex shedding during the steady state calculations a very low maximum residual (1E-6) convergence criteria is applied, otherwise greatly elongated Foppl vortices are predicted rather than allowing the vortices to detach and oscillate in a quasi-realistic manner. In a steady state calculation the solver does not converge to a steady solution, rather it cycles through flow configurations similar to vortex shedding.

Once the steady state calculation begins to cycle it is stopped and a transient simulation is started from the quasi-steady-state solution. The following steps are followed for each time step.

1) The position of the tube is confirmed at the beginning of the time step by calculating the coordinates of the tube center from any three co-planar points on the tube surface.
2) The pressure and shear forces are calculated at each node on the surface of the tube.
3) The forces are then integrated around the surface of the tube to calculate the net lift and drag forces acting on the tube.
4) The lift and drag forces and current tube position are passed to the structural code, which uses the Central Difference Method to solve the equation of motion for the tube and returns a new tube position to the main program.
5) The old position is subtracted from the new position to determine the net movement of the tube and the tube surface nodes (the 'moved-nodes' region) are moved accordingly.
6) The 'frozen nodes' region is held static and the displacement of the 'moved nodes' region is diffused through the rest of the grid using a Laplacian diffusion solution.
7) The momentum equations, and turbulence equations as needed, are solved in ALE form by subtracting the grid velocity from the advecting flow field velocity.
8) The simulation advances to the next time step. There is no grid adjustment during the coefficient iterations within a time step.

Model Validation

The primary controllable parameters limiting the accuracy of the tube model are the grid density, the time step, and in particular the blockage ratio which is defined as the ratio of domain width to tube diameter. These variables, along with CFD discretization parameters were tested to provide a tested rigid static tube model from which the elastic tube / moving grid solution could be subsequently run.

Validation Criteria

Preliminary validation of the model consists of matching the mean and RMS drag coefficient, RMS lift coefficient and Strouhal number to experimental data [6]. The instantaneous drag coefficient (C_D) and lift coefficient (C_L) are calculated from the instantaneous drag force (F_D) and lift force (F_L) as follows.

$$C_D = \frac{2F_D}{\rho U^2 d} \quad C_L = \frac{2F_L}{\rho U^2 d}$$

where ρ is the fluid density (1.164 kg/m^3), d is the tube diameter (0.016 m) and U is the free stream velocity (0.09794 m/s) for a Reynolds number of 100. The Strouhal number (St) is a dimensionless number relating vortex shedding frequency f, tube diameter and mean fluid velocity:

$$St = \frac{fd}{U}$$

Initially various discretization schemes were investigated to determine a suitable scheme to be used in the node number and time step tests. In this case, with relatively strong counter-currents in the vortex recirculation zone, the Modified Linear Profile scheme (MLP) with Physical Advection Correction (PAC) proved most effective at reproducing experimental results (See CFX-TASCflow Theory [4] details on discretization schemes).

A qualitative check was initially made on the predicted results at a Reynolds number of 100. Due to the nature of vortex shedding, the lift force oscillates about zero at a frequency equal to the Strouhal frequency. The drag force will oscillate about some positive value at a frequency twice the Strouhal frequency. Figure 3 shows the predicted drag and lift forces, and resultant Strouhal frequency for a rigid tube at Reynolds number 100. The prediction exhibits the correct frequency behaviour, with $C_{L\text{-}Mean} = 0$, $C_{L\text{-}RMS} > 0$ and $C_{D\text{-}Mean} > 0$. A typical flow field is also shown in Figure 4, consisting of a vorticity contour plot overlaid on a pressure fringe plot. These show low pressure zones near the centers of the each vortex and the oscillating nature of the flow. To improve clarity, the vorticity contours upstream of the tube have been omitted.

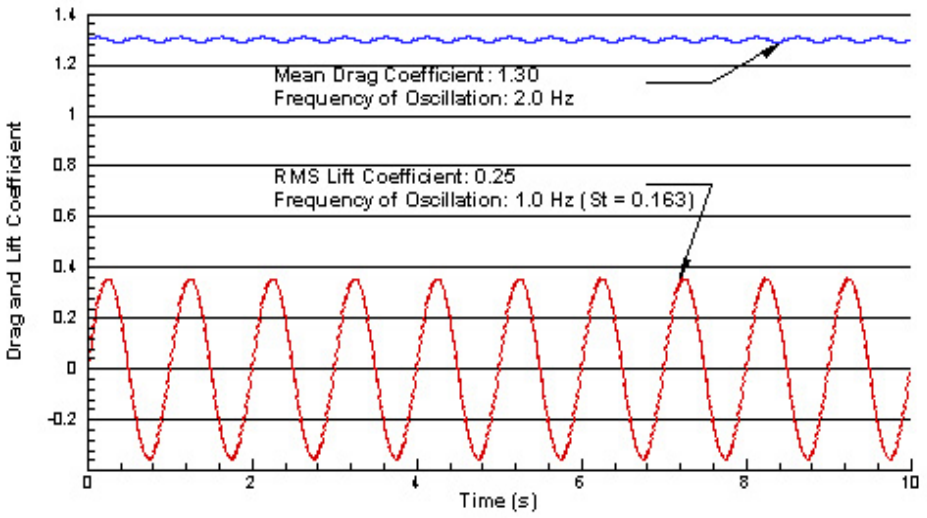

Figure 3. Expected Lift/Drag Coefficient History, Re = 100

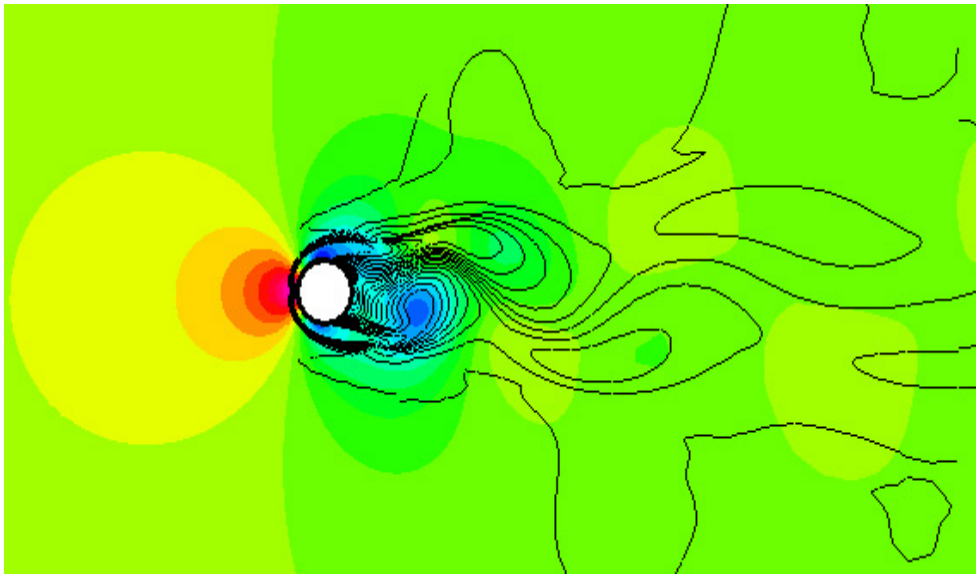

Figure 4. Rigid Tube Flow Visualization

Blockage Influence

The first step in generating the model consists of selecting a domain size. The initial domain was sized at 11 diameters wide with the tube at the center, giving a blockage ratio of 11. The inlet was placed 8 diameters upstream and the outlet was placed 20 diameters downstream from the tube.

Two shortcomings of this domain were revealed.

1) Due to the relatively slow flow velocity, pressure information propagates readily upstream. It was discovered that the initial domain was too short to prevent the outlet constant pressure condition from interfering with the flow around the tube, and the pressure effects from the stagnation point at the tube were being propagated to the inlet. The outlet boundary condition was particularly responsible for a non-converging solution.

2) Investigation of past research revealed that a narrow domain may not interfere significantly with the lift and drag forces on the tube, but the vortex shedding frequency is highly dependant on the blockage ratio, defined as the free flow area adjacent the tube normalized by the diameter of the tube. Stansby and Slaouti demonstrated that low blockage ratios have the effect of increasing the Strouhal number and hence vortex shedding frequency [6].

To address these two issues the domain dimensions were increased to those shown in Figure 2 where the blockage ratio is increased to 21 and the upstream and downstream boundaries are located at 13 and 59 diameters respectively. The choice of blockage ratio was based on the findings in [6].

Grid Sensitivity Studies

Since the flow features around the tube were of primary interest, in particular the flow separation point and subsequent recirculation regions, nodes were concentrated around the tube and in the immediate downstream flow area. This resulted in some elements with a very narrow aspect ratio, however these were concentrated near the walls. The final near-tube grid consists of 360 circumferential nodes and 40 radial nodes within roughly 1 diameter of the tube.

Figure 5 shows the dependence of the solution on circumferential node number at the tube surface. The final mesh can be seen in Figure 6.

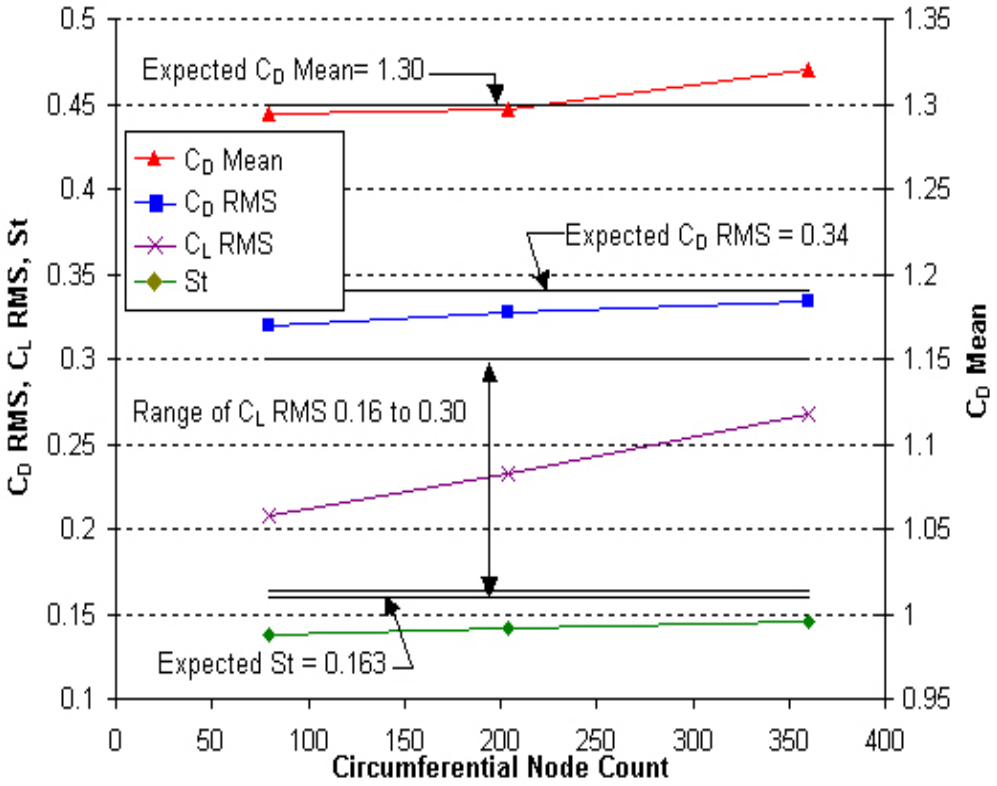

Figure 5. Circumferential Node Number Dependence of Solution (Re = 100, Timestep = 0.005 seconds)

With 360 circumferential nodes, the mean and RMS drag are within 2% of experimental values. There is a significant change in the RMS lift from 204 nodes to 360, however in both cases the value falls within 7% of a typical value at this Reynolds number. Experiments have demonstrated that significant variations in lift coefficient exist at low Reynolds number [7] and the results of both simulations are considered acceptable. The Strouhal number is within 11% of available experimental results and this is considered adequate given the experimental uncertainty associated with low Reynolds number flows. While finer grid resolutions could be examined, for practical simulation time limits the results are within an acceptable range.

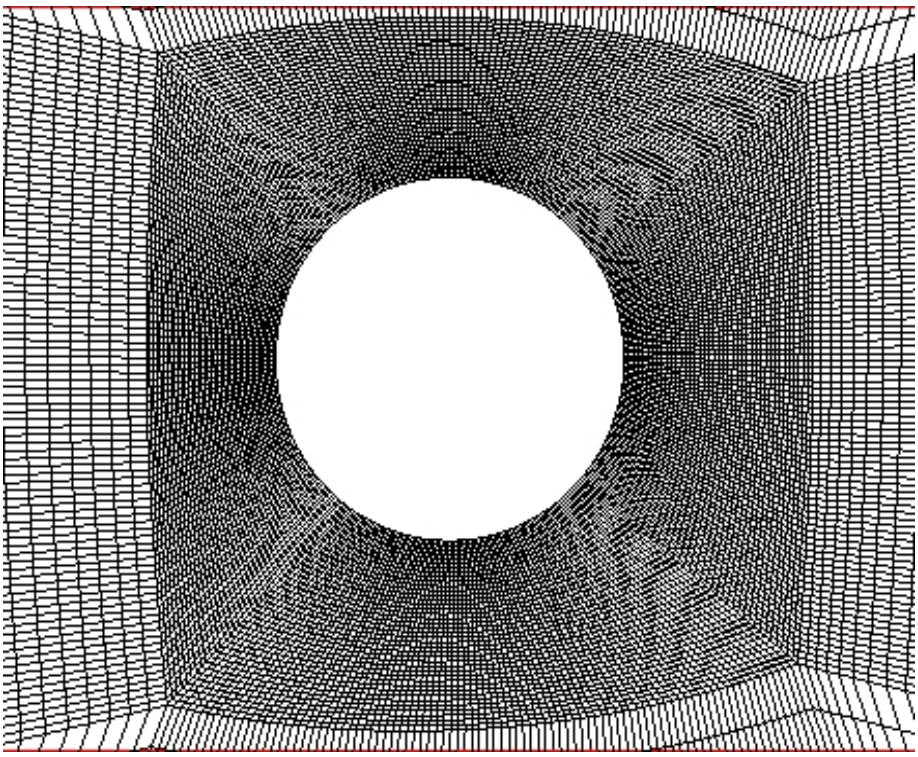

Figure 6. Final Grid at Tube

Time Step Validation

Having set the domain with 360 circumferential nodes, the solution dependence on time step was investigated. The second-order transient scheme was used for the rigid tube case. This scheme reduces solution error quadratically with linear time step reduction. The expected vortex shedding frequency was approximately 1 Hz (for Re=100). As a result, the initial time step chosen was 0.1 seconds, which would provide 10 sample points per vortex shedding cycle, or roughly 5 sample points per half-cycle. This proved to be a large time step, which cannot accurately reproduce experimental results. Therefore the time step was reduced until the accuracy improved as shown in Figure 7. The final time step used for a Reynolds number of 100 is 0.02 seconds, giving roughly 50 sample points per vortex shedding cycle.

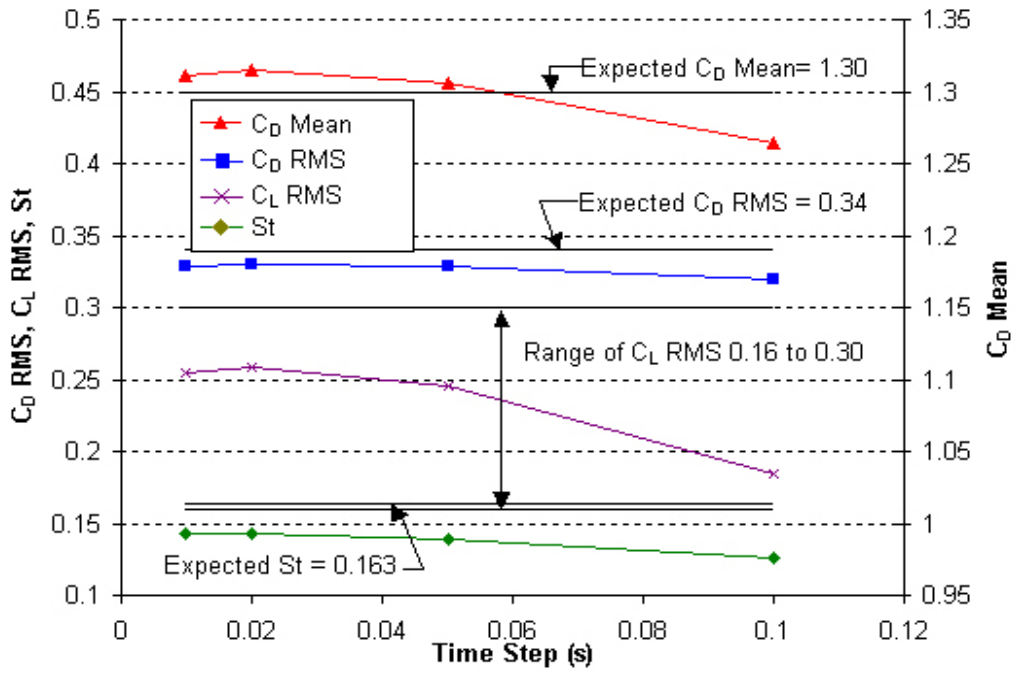

Figure 7. Time Step Dependence (Re = 100, Grid Res: 204 circ. nodes)

Results

Having validated the model for a rigid tube, the moving grid algorithm was activated. Results are subsequently shown for three Reynolds numbers, the first in a laminar regime, the second with turbulent flow, and the third with turbulent flow near resonance conditions.

Figure 8 shows the response of the tube at Reynolds number 100. The free stream velocity is 0.098 m/s. The simulation is begun with an un-displaced tube in a quasi-steady flow field that has been initially obtained. As shown, the tube response displays a transient response at the natural frequency of 30 Hz which is eventually damped out and the tube follows the fluid forces and vibrates at the Strouhal frequency in the lift direction (red line) and at twice the Strouhal frequency in the drag direction (blue line) as expected. Once the natural response has declined, the peak deflection in the lift direction is 6.88E-9 m which is approximately the static response expected for the peak lift force of 29.8E-6 N. The mean deflection in the drag direction is 20.3E-9 m, which corresponds to the peak drag force of 88.0E-6 N. These are very small deflections and forces corresponding to a very low Reynolds number. They would not be detectible in practice.

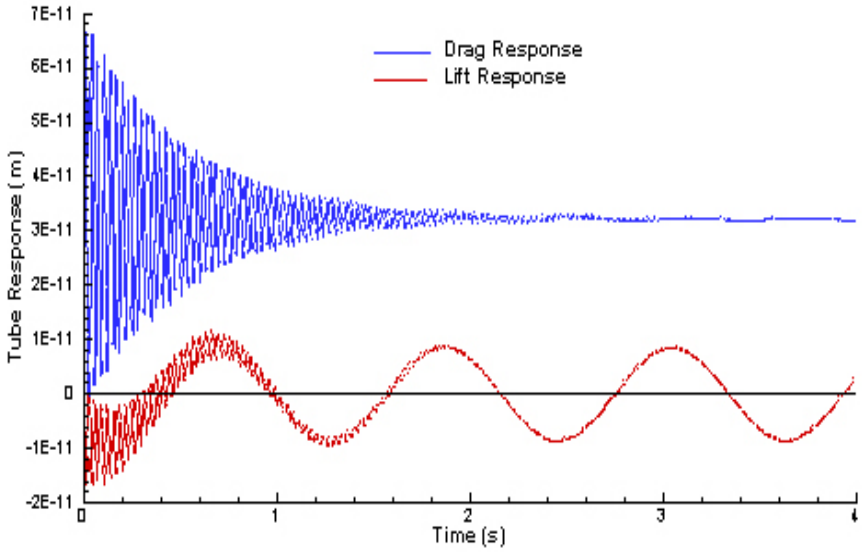

Figure 8. Tube Response: Reynolds No = 100 (dt = 0.02, Grid Res: 360 circ. nodes)

Figure 9 shows the elastic response at a Reynolds number of 1000. The free stream velocity is 0.979 m/s. In this case the Strouhal frequency is approximately one third the natural frequency. Once the transient response dies out, it is apparent the tube is vibrating at the Strouhal frequency and in phase with the lift and drag forces. The mean drag and peak lift deflections are 2.28E-6 m and 3.00E-6 m respectively. These represent increases in displacement amplitude of two orders of magnitude in the drag direction and three in the lift direction for a single order of magnitude increase in Reynolds number. The peak displacement in the lift direction exceeds mean displacement in the drag direction at the relatively slow flow velocity.

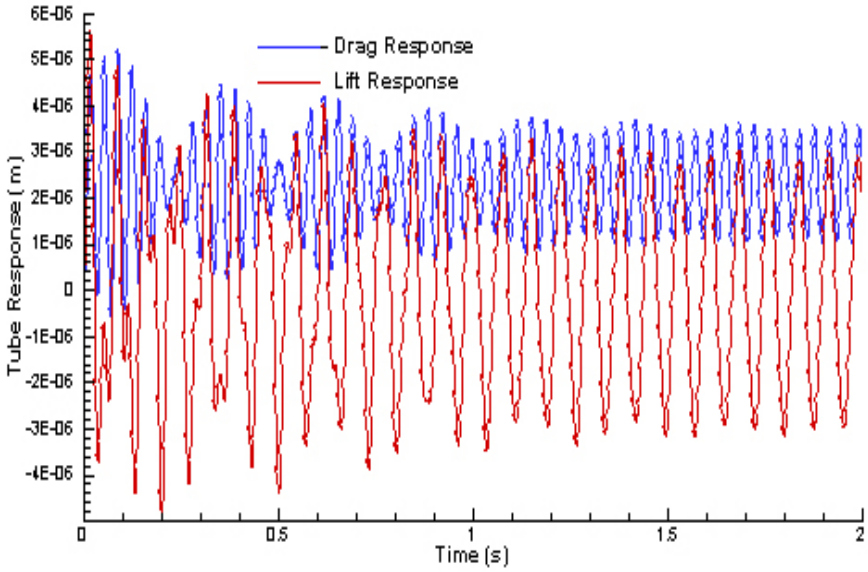

Figure 9. Tube Response: Reynolds No = 1000 (dt = 0.002, Grid Res: 360 circ. nodes)

Figure 10 shows the elastic response of the tube at a Reynolds number of 2450. Here the Strouhal frequency is nearly equal to the natural frequency of the tube and the effects of resonance can be observed. For a simulation time, the same as at a Reynolds number of 1000, we obtain a stronger tube response. Assuming the tube will respond by overshooting its steady-state peak response and then steady out, a simple analysis of the available data is possible. The amplitude of vibration in the lift direction is much greater than at a Reynolds number of 1000. The current data shows the tube response nearing its first peak. The maximum response here is approximately 600E-6 m and is an order of magnitude larger than the drag displacement. This represents a two order of magnitude increase in vibration amplitude from a 145% increase in free stream velocity. Once again, the tube is vibrating at the Strouhal frequency.

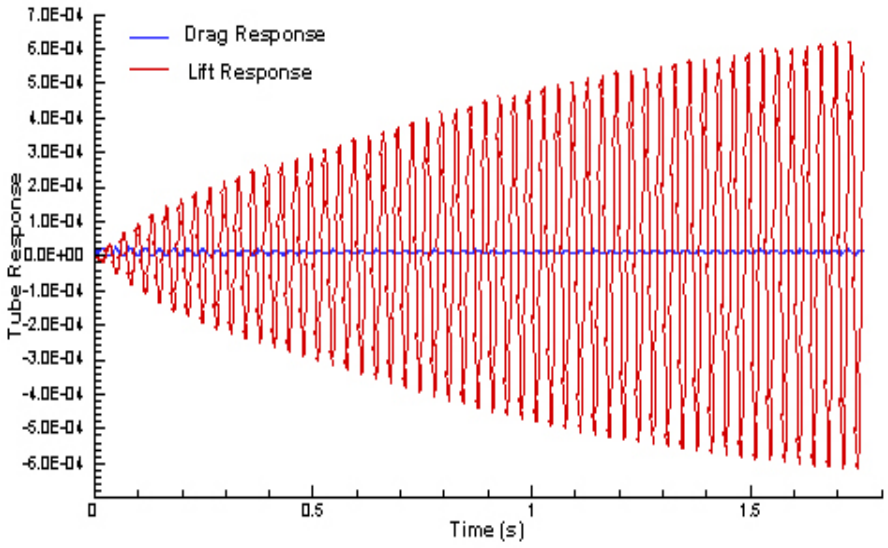

Figure 10. Tube Response: Reynolds No = 2450 (dt = 0.001, Grid Res: 360 circ. nodes)

Conclusion

The structural response of a single elastic tube has been successfully simulated at various Reynolds numbers by coupling fluid flow predictions obtained using CFX-TASCflow to a dynamic tube response model which calculates the tube displacement from fluid forces. The ALE moving grid algorithm was used to apply the tube displacements to the CFD solution.

The model has been validated by comparing results of a rigid cylinder in the form of RMS and mean drag coefficient, RMS lift coefficient and Strouhal number, to typical experimental values. The elastic tube model has been validated qualitatively by comparing the simulated response to the expected response characteristics of an elastic tube at various Reynolds numbers including a near-resonance simulation. The model has realistically predicted the natural and forced response of the tube and reproduced the amplitude intensifying effects of resonance.

Future work will include modifying the model to produce greater displacements, simulating arrays of elastic tubes, and extracting the coefficients required to complete the Unsteady Flow Theory model for fluidelastic instability.

References

1) S.S. Chen 1987, A General Theory for Dynamic Instability of Tube Arrays in Corssflow, Journal of Fluids and Structures **1**, 35-53.

2) H. Tanaka, S. Takahara 1981, Fluid Elastic Virbration of Tube Array in Cross Flow, Journal of Sound and Vibration **77**, 19-37.

3) C.W. Hirt, A.A Amsden, J.L. Cook 1974, An Arbitrary Lagrangian-Eulerian Computing Method for all Flow Speeds, Journal of Computing Physics **14**, 227 - 253.

4) "CFX-TASCflow Theory, V2.12.1", ANSYS Canada, 2002.

5) C.H.K. Williamson 1991, 2-D and 3-D Aspects of the Wake of a Cylinder, and their Relation to Wake Computations, Lectures of Applied Mathematics **28**, 719 - 751. Providence, RI: American Mathematical Society.

6) P.K. Stansby, A. Slaouti 1993, Simulation of Vortex Shedding Including Blockage by the Random-Vortex and Other Methods, International Journal for Numerical Methods in Fluids **17**, 1003-1013.

7) C. Norberg 2001, Flow Around a Circular Cylinder: Aspects of Fluctuating Lift, Journal of Fluids and Structures **15**, 459-469.